Dynamic and Static Light Scattering on Aqueous Solutions of Sodium Alginate

Knut Arne Strand,*,† Arild Bøe,†,§ Peer Staale Dalberg,†,‖ Torbjørn Sikkeland,*,† and Olav Smidsrød‡

Division of Experimental Physics and Division of Marine Biochemistry, University of Trondheim, N-7034 Trondheim-NTH, Norway. *Received August 11, 1980*

ABSTRACT: Dynamic and static light scattering experiments have been performed at room temperature on sodium alginate ($\langle M \rangle_w = 1.9 \times 10^5$) in the concentration range 0.2–2 g/L and in the ionic strength range 4.4–95 mM. By the introduction of a simple method based on the Schwarz inequality we have (1) compared various moments for the distribution of the radius of gyration and of the molecular weight, (2) obtained the value 10 ± 6 nm for the Kuhn statistical segment, and (3) obtained from both diffusion and viscosity measurements values for equivalent-sphere parameters, which, within large errors, are in agreement with predictions by the Kirkwood–Riseman theory. Interaction properties as reflected in the values for virial coefficients and in the shapes of the photon correlation functions are discussed.

I. Introduction

Alginates, which comprise the intercellular substance in brown algae, are used in industry mainly because of their ability to form viscous solutions, to bind divalent metal ions, and to form gels. The alginates have been shown to be composed of 1,4′-linked residues of β-D-mannuronic and α-L-guluronic acid in varying proportions.[1,2]

Physical properties of sodium alginate in dilute aqueous solutions have previously been studied by static light scattering, osmotic pressure, and viscosity measurements.[1-3] With the assumption that the molecular weights have a Schulz distribution,[4,5] analysis of the data from such measurements has indicated that the molecules can be described as very extended random coils with partially free drainage.[1]

In the present work we apply static as well as dynamic light scattering techniques. In the former, one extracts average values for the molecular weight, M, radius of gyration, R_G, and the virial coefficient, B_2, and in the latter, values for the average and the variance of the translational diffusion coefficient, D^e, and the virial coefficient, B_D, for diffusion. These quantities are measured at room temperature, and as variables we use the concentration of the alginate, c, the ionic strength, I, and scattering angle, θ.

The object is to obtain information on both single-particle properties and interaction properties. We test the validity of using the Schulz distribution on the alginate molecular weights. By using a simple method based on the Schwarz inequality and assuming that[6] $D^e \propto 1/R_G$, we obtain values for ratios for various moments in the distribution of both R_G and M. This method also yields values for parameters describing the extension and drainage of the alginate molecules without any assumption on the molecular weight distribution.

In analyzing the effect of electrostatic interaction on B_2, we apply the model of Nagasawa and Takahashi.[7] We attempt to obtain information on interaction effects also by analyzing the long-time behavior of the correlation function by using the so-called "cage" model.[8]

The paper is organized as follows. In section II we briefly outline the procedure for the sample preparation, the experimental setups, and the methods, including the cage model, used to analyze the light scattering data. Values for various relevant quantities are presented. In section III we analyze the effects of polydispersity and particle interaction on these quantities.

II. Experimental Methods and Results

Sample Preparations. For the experiments in the present work we used sodium alginate from *Laminaria digitata* harvested at Tarva, Norway, Aug 29, 1961. Following a procedure described by Haug,[2] we extracted the alginate from seaweed as sodium alginate and stored it in the dried state until use. In this alginate the ratio between mannuronic and guluronic acid residues was 1.60 and 1.56 according to chemical analysis[2] and ^{13}C NMR studies,[9] respectively.

The solutions were prepared as described in ref 10 and 11. To prevent bacterial growth two drops of toluene per liter was added. To avoid aggregation the solutions were made with an admixture of 1 mM NaEDTA, a chelating agent which binds divalent ions present as an impurity in the alginate. The solutions were clarified by centrifuging for 2 h at 200000g followed by gentle suction through a 0.2-μm Unipore filter directly into the light scattering cell. This cell was then inspected for dust by using a He–Ne laser beam in conjunction with a microscope with magnification 16×. If more than a few dust particles were observed in the field of view, the solution was refiltered. Despite this procedure there always were some dust particles left in the sample, which constituted the main contribution to the uncertainty in both our static and dynamic measurements.

The concentration of the alginate ranged from a lower detection limit (0.2 g/L), set by our dynamic light scattering setup, to an upper limit (2 g/L), above which filtering becomes cumbersome. For the ionic strength the lower limit (4.4 mM) was set by the concentration of EDTA and the upper limit (95 mM) was chosen to be close to the value used in earlier static light scattering studies.[3,10]

The alginate concentration was determined by use of the phenol–sulfuric acid color reaction.[2,10]

For each of the solutions the pH was 6.3 ± 0.1. Since the alginate itself has some buffer capacity at this pH level, no other buffer was introduced.

The light scattering experiments were performed within 1 week from the dissolution of the alginate. A separate experiment indicated that over a period of 2 weeks no change took place in either the static or the dynamic light scattering properties of a solution. Hence, our results are not disturbed by aging effects.

Since the average size of the alginate molecules varies from one extraction to another, all measurements were

† Division of Experimental Physics.
‡ Division of Marine Biochemistry.
§ Present address: Rogalandsforskning, Ullandhaug, N-4001 Stavanger, Norway.
‖ Present address: Det norske Veritas, Veritasvn. 1, N-1322 Høvik, Norway.

0024-9297/82/2215-0570$01.25/0

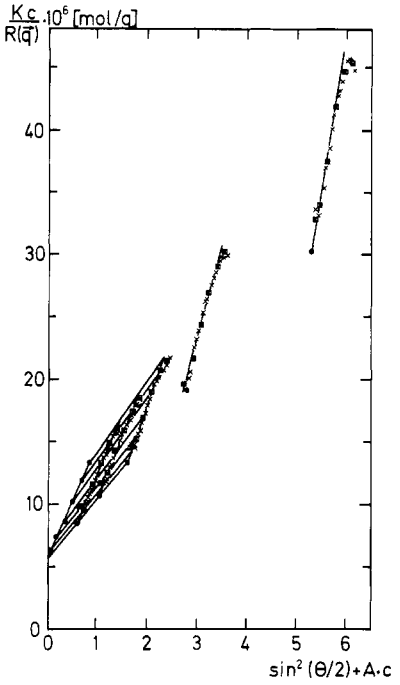

Figure 1. Example of a Zimm plot. The data are taken from a measurement on alginate in 10 mM NaCl and 1 mM NaEDTA. The constant A is chosen to be equal to 5 L/g. The smooth curves are drawn by eye. For clarity, error bars have been omitted. Typical errors for extrapolated values are shown in Figure 2.

performed on samples from one extraction.

Static Light Scattering. The conventional light scattering experiments were performed with a commercial Brice-Phoenix OM-2000 light scattering photometer.[12]

The time-averaged scattered intensity, $I(q)$, corrected for the scattering from the pure solvent, was measured as a function of scattering angle at various concentrations and ionic strengths. The experimental data were analyzed in a conventional way by using a Zimm plot.[13] An example of such a plot is shown in Figure 1, in which the quantity $Kc/R(q)$ is plotted vs. $\sin^2(\theta/2) + Ac$, where A is an arbitrary constant and the parameter K is[14]

$$K = 2\pi^2 n_0^2 \left(\frac{dn}{dc}\right)^2 / (N_A \lambda_0^4) \qquad \text{(II.1)}$$

Here, n_0 is the index of refraction of the solvent, dn/dc is the refractive index increment of the solution, for which we used the value 1.5×10^{-2} L/g as taken from ref 3, N_A is Avogadro's number, and λ_0 is the wavelength of the light in a vacuum. $R(q)$ is the Rayleigh ratio, which for unpolarized incident light is given by

$$R(q) = \frac{I(q)r^2}{I_0 V(1 + \cos^2\theta)} \qquad \text{(II.2)}$$

where $\vec{q} \equiv \vec{k}_i - \vec{k}_f$ is the scattering vector, V is the scattering volume, r is the distance from that volume to the detector, and I_0 is the intensity of the incident beam. In the quasi-elastic approximation $|\vec{k}_f| \approx |\vec{k}_i|$ and $q = |\vec{q}| = (4\pi n/\lambda_0) \sin(\theta/2)$.

For the monodisperse sample of flexible coils Zimm[13] has developed the following expression for the quantity $Kc/R(q)$:

$$\frac{Kc}{R(q)} \approx \frac{1}{MP(q)} + 2B_2c \qquad \text{(II.3)}$$

Here, B_2 is the static virial coefficient and $P(q)$ is the single-particle form factor.[14] When $qR_G \ll 1$, $P(q)^{-1}$ can be approximated by $1 + q^2R_G^2/3$.[15] Then when the polarizability of a scatterer is independent of its molecular weight, it is easy to show[14] that for a polydisperse sample

$$\frac{Kc}{R(q)} \approx \frac{1}{\langle M\rangle_w}\left(1 + \frac{q^2\langle R_G^2\rangle_z}{3}\right) + 2B_2c \qquad \text{(II.4)}$$

Here, $\langle\ \rangle_w$ denotes weight average, $\langle\ \rangle_z$ denotes the z average (average weighted with the square of the molecular weight), and B_2 represents the virial coefficient of the polydisperse system.

Since the alginate molecules are highly charged, they may not be well described by the model of Zimm.[13] We shall, however, only make use of values for $Kc/R(q)$ extrapolated to $c = 0$ or $q = 0$. For that purpose eq II.4 should in any case be adequate.

We must also point out that eq II.4 is derived for a two-component system. According to ref 7 it is, however, still valid when a neutral salt is present, provided the sample solution is dialyzed to equilibrium with the solvent containing the salt and the quantity dn/dc is measured between these dialyzed solutions.

Analyzing the Zimm plots according to eq II.4, we obtained

$$\langle M\rangle_w = (1.9 \pm 0.2) \times 10^5 \qquad \text{(II.5)}$$

independent of ionic strength and

$$\langle R_G^2\rangle_z^{1/2} = 50 \pm 7 \text{ nm} \qquad \text{(II.6)}$$

for our four highest ionic strengths ($I = 95$ mM to $I = 14$ mM). At the lowest ionic strength ($I = 4.4$ mM) the extrapolation to $c = 0$ was too uncertain to yield a meaningful value for $\langle R_G^2\rangle_z^{1/2}$.

In Figure 2 we have plotted experimental values for $Kc/R(0)$ vs. concentration. The initial linear slopes are indicated, from which values for $2B_2$ and $1/\langle M\rangle_w$ are extracted. The former, in the form of $2B_2\langle M\rangle_w$, is plotted vs. $1/I$ in Figure 3. This plot suggests a linear relationship

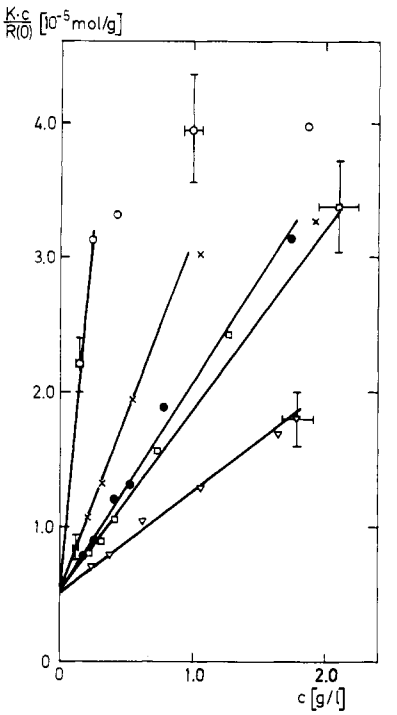

Figure 2. $Kc/R(0)$ as a function of concentration for alginate in solutions of 1 mM NaEDTA and 91 mM NaCl (▽), 1 mM NaEDTA and 50 mM NaCl (□), 1 mM NaEDTA and 30 mM NaCl (●), 1 mM NaEDTA and 10 mM NaCl (×), and in 1 mM NaEDTA (○). The error bars include conservatively assessed systematic errors. The straight lines are drawn by eye.

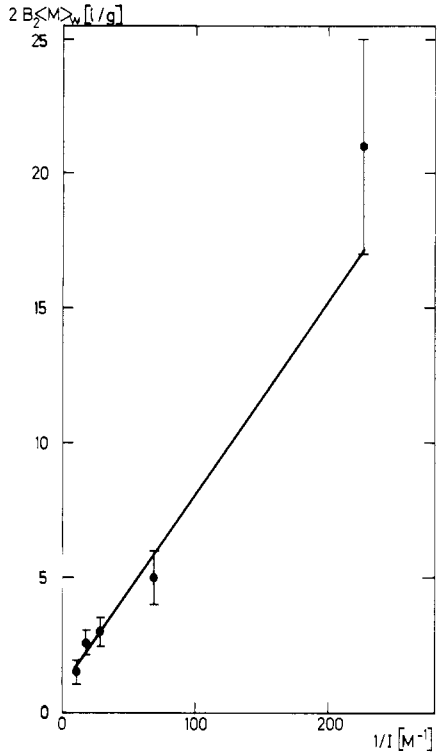

Figure 3. Static virial coefficient as a function of $1/I$. The error bars include conservatively assessed systematic errors and hence the straight line drawn by eye is inside all the bars.

between B_2 and $1/I$ as discussed in section III.

Our value 1.5 ± 0.5 L/g for $2B_2\langle M\rangle_w$ at I = 95 mM is in agreement with the value 1.8 L/g obtained by Dingsøyr and Smidsrød[11] for a similar alginate sample at I = 100 mM.

Figure 2 shows that at the lowest ionic strengths there is a leveling off at the highest concentration not accounted for by eq II.4. This effect is considered in section III.

Dynamic Light Scattering. A schematic diagram of the spectrometer used for the dynamic light scattering experiments is shown in Figure 4. We used a Spectra-Physics argon ion laser (Model 165-03) as the light source and chose the green line (λ_0 = 514.5 nm) since this yields the highest power (1.4 W). To obtain sufficient intensity a lens with focal length 60 cm was introduced to focus the laser beam in the scattering volume. The intensity of the incident laser beam was measured with a power meter (UDT 122A with integrating sphere Model 2500).

A Glan polarizing prism (B. Halle, extinction ratio better than 10^{-5}) was used to improve the polarization of the laser beam. To measure the depolarization ratio of the scattered light a second polarizer (P_2) was introduced.

To obtain refractive index matching and temperature control, the scattering cell (Brice-Phoenix C-101) was placed in a temperature-controlled water bath. The measurements were performed at room temperature, and experimental values for the diffusion coefficients were referred to 20 °C by the usual temperature/viscosity correction.

The intensity of the scattered light was measured by using an ITT FW-130 photomultiplier, which was specially selected for a low dark counting rate and a low degree of self-correlation. To obtain spatial coherence[16] two apertures and a lens were placed in front of the photomultiplier as shown in Figure 4.

The signal from the photomultiplier was passed to the correlator through a discriminator–standardizer (Malvern Instruments RR63). The correlator (Malvern Instruments

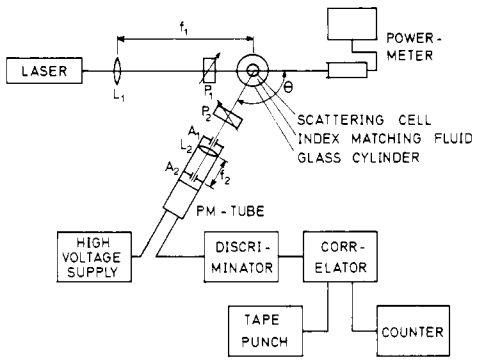

Figure 4. Schematic diagram of the spectrometer. P_1 and P_2 are polarizers. A_1 and A_2 are apertures, both with diameter 0.3 mm. L_1 and L_2 are lenses with focal lengths f_1 = 60 cm and f_2 = 12 cm and with focal points in the scattering volume and the aperture A_2, respectively. θ is the scattering angle, which may be varied between 30 and 130°.

24-channel digital autocorrelator) was operated in the single-clipped autocorrelation mode.[16]

The measurements were performed at 6–8 different angular positions in the range 30–130°. The concentrations of the solutions were so low that the effect of multiple scattering could be ignored.

The setup was checked for systematic erros due to fluctuations in the light intensity from the laser, vibrations, and self-correlation in the photomultiplier by measuring the intensity correlation function of fluorescence from a fluorescence standard (Applied Photophysics) which emits light around 560 nm when excited at 514.5 nm. The normalized intensity correlation function of the fluorescence was found to deviate less than 0.4% from 1 in the time range of interest, indicating that self-correlations in the spectrometer were negligible. The performance of the dynamic light scattering setup was further checked by measuring the translational diffusion coefficient of bovine serum albumin (BSA, Sigma fraction V) in 150 mM KCl, 8 mM phosphate buffer (pH 7.6) at 20 °C, which was found to be (5.9 ± 0.1) × 10^{-11} m^2/s, in close agreement with the results reported by others.[17]

Employing the thermal lens effect described by Gordon et al.,[18] we found the local temperature rise due to absorption of the laser beam to be less than about 0.2 °C.

The relation between the experimental, normalized, single-clipped photon correlation function, $g_k^{(2)}(\tau,t_s)$, and the normalized field correlation (NFC) function of first order, $g^{(1)}(q,\tau)$, is[16]

$$g_k^{(2)}(\tau,t_s) = 1 + b|g^{(1)}(q,\tau)|^2 \qquad \text{(II.7)}$$

where t_s is the sampling time, $\tau = t_s, 2t_s, \ldots, 24t_s$, and b is a constant which is treated as an experimental parameter as discussed in more detail in ref 16.

In Figure 5 are shown examples of autocorrelation functions, where the quantity $\ln(b^{1/2}|g^{(1)}(q,\tau)|)$ is plotted vs. τ. Using a method introduced in ref 8, we obtained values for both the average, $\langle\Gamma(\tau_0)\rangle$, and the variance, Var $(\Gamma(\tau_0))$, of the decay constant $\Gamma(\tau_0)$ of the NFC function at $\tau = \tau_0$. Their values at $\tau_0 = 0$ shall be denoted by $\langle\Gamma\rangle$ and Var (Γ), respectively.

We first consider the q^2 dependence of the quantities $\langle\Gamma\rangle/q_2$ and Var $(\Gamma)/q^4$. Typical examples are shown in Figures 6 and 7. Both $\langle\Gamma\rangle/q^2$ and Var $(\Gamma)/q^4$ depend on q. This dependence might be due to both interaction effects and polydispersity.

The effect of polydispersity has been considered by Brehm and Bloomfield[19] and by Strand and Sikkeland.[20] When the single-particle form factor $P(q)$ can be approx-

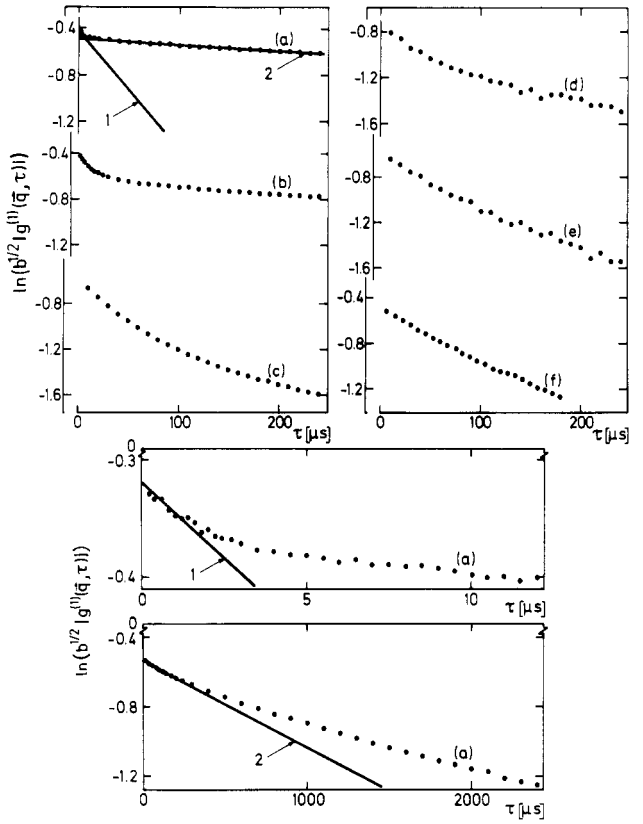

Figure 5. $\ln (b^{1/2}|g^{(1)}(q,\tau)|)$ as a function of τ for $\theta = 90°$ for various concentrations and ionic strengths: (a) $c = 1.9$ g/L, $I = 4.4$ mM; (b) $c = 1.9$ g/L, $I = 14$ mM; (c) $c = 1.7$ g/L, $I = 95$ mM; (d) $c = 0.26$ g/L, $I = 4.4$ mM; (e) $c = 0.21$ g/L, $I = 14$ mM; (f) $c = 0.24$ g/L, $I = 95$ mM. The straight lines fitted to curve a indicate initial (1) and long-time (2) slopes of $\ln |g^{(1)}(\bar{q},\tau)|$.

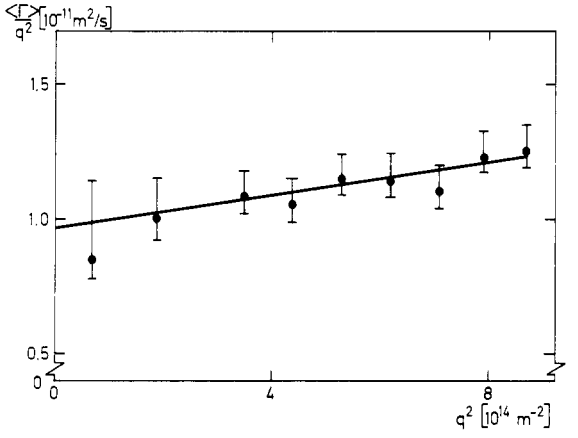

Figure 6. $\langle\Gamma\rangle/q^2$ plotted as a function of q^2 for a solution of 0.24 g/L alginate in 91 mM NaCl and 1 mM NaEDTA. The error bars include conservatively assessed systematic errors and hence the straight line drawn by eye is within all the bars.

imated by $1 - q^2R_G^2/3$ and interaction does not influence the q dependence, the following expressions are valid:[20]

$$\frac{\langle\Gamma\rangle}{q^2} \approx \langle D^e\rangle_z + \frac{q^2}{3}(\langle D^e\rangle_z\langle R_G^2\rangle_z - \langle D^e R_G^2\rangle_z) \quad \text{(II.8)}$$

and

$$\frac{\text{Var }(\Gamma)}{q^4} \approx \langle (D^e)^2\rangle_z - \langle D^e\rangle_z^2 + \frac{q^2}{3}(\langle (D^e)^2\rangle_z\langle R_G^2\rangle_z - \langle (D^e)^2 R_G^2\rangle_z - 2\langle D^e\rangle_z^2\langle R_G^2\rangle_z + 2\langle D^e\rangle_z\langle D^e R_G^2\rangle_z) \quad \text{(II.9)}$$

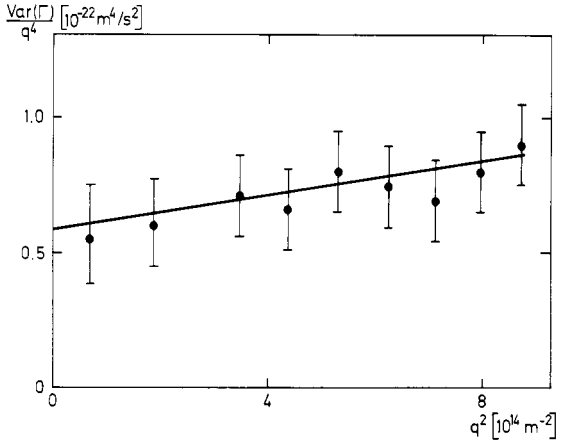

Figure 7. Var $(\Gamma)/q^4$ as a function of q^2 for a solution of 0.24 g/L alginate in 91 mM NaCl and 1 mM NaEDTA. The error bars include conservatively assessed systematic errors and hence the straight line drawn by eye is within all the bars.

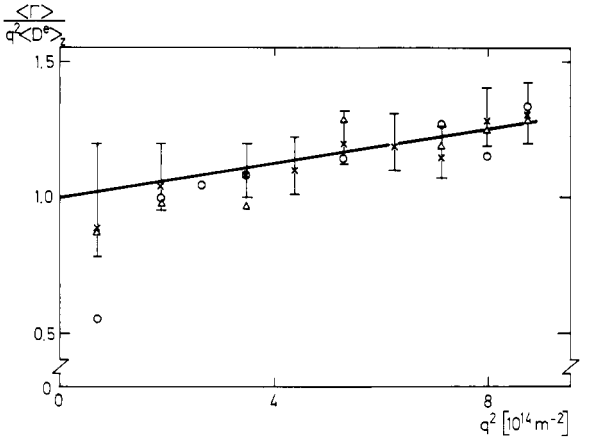

Figure 8. $\langle D^e\rangle_z^{-1}\langle\Gamma\rangle/q^2$ as a function of q^2 for (a) 0.24 g/L alginate in 91 mM NaCl and 1 mM NaEDTA (×), 0.32 g/L alginate in 10 mM NaCl and 1 mM NaEDTA (△), and (c) 1.9 g/L alginate in 10 mM NaCl and 1 mM NaEDTA (○). The straight line represents the mean value for all the samples used in the present work. The error bars given include conservatively assessed systematic errors.

To discuss the q dependence of $\langle\Gamma\rangle/q^2$, it is instructive to consider the quantity $\langle D^e\rangle_z^{-1}\,\partial(\langle\Gamma\rangle/q^2)/\partial q^2$. In Figure 8 we have plotted values for the quantity $\langle D^e\rangle_z^{-1}\langle\Gamma\rangle/q^2$ vs. q^2 for three different samples. For all c and I we found that this quantity, within error, shows the same linear q^2 dependence and the slope to be given by

$$\frac{1}{\langle D^e\rangle_z}\frac{\partial}{\partial q^2}\left(\frac{\langle\Gamma\rangle}{q^2}\right) = (3.1 \pm 0.5) \times 10^{-16}\ \text{m}^2 \quad \text{(II.10)}$$

which is apparently also valid at $c = 0$, where there is no interaction. Hence, since internal motion can be neglected[21] in the examined q region ($q\langle R_G^2\rangle_z^{1/2} < 1.4$), the value given by eq II.10 may entirely be ascribed to the effect of polydispersity.

The example of the q^2 dependence of Var $(\Gamma)/q^4$ shown in Figure 7 is taken from the sample with the lowest concentration and the highest ionic strength ($c = 0.24$ g/L, $I = 95$ mM), for which the interaction is weak, and hence the variance is expected to be mainly due to polydispersity. For this sample the value of the quantity $\langle (D^e - \langle D^e\rangle_z)^2\rangle_z$ determined according to eq II.9 is $(0.58 \pm 0.10) \times 10^{-22}$ m^4/s^2. This value in conjunction with the value $\langle D^e\rangle_z = (0.96 \pm 0.07) \times 10^{-11}$ m^2/s as taken from Figure 6 gives

$$\langle\langle (D^e - \langle D^e\rangle_z)^2\rangle_z\rangle^{1/2}/\langle D^e\rangle_z = 0.8 \pm 0.1 \quad \text{(II.11)}$$

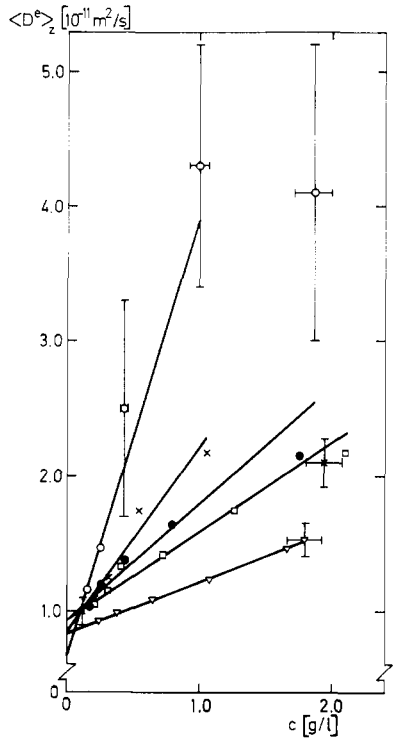

Figure 9. Effective diffusion coefficient referred to 20 °C as a function of concentration for alginate in solutions of 1 mM NaEDTA and 91 mM NaCl (▽), 1 mM NaEDTA and 50 mM NaCl (□), 1 mM NaEDTA and 30 mM NaCl (●), 1 mM NaEDTA and 10 mM NaCl (×), and 1 mM NaEDTA (○). The error bars include conservatively assessed systematic errors. The straight lines are drawn by eye.

Within uncertainty, the same value for this quantity was obtained for two samples at higher concentrations (c = 0.37 and 0.64 g/L) and at the same ionic strength. This suggests that the variance in D^e is entirely due to polydispersity and that the effect of interaction can be ignored.

In Figure 9 we have plotted $\langle D^e \rangle_z$, determined according to eq II.8, as a function of concentration. The initial linear slopes are indicated, from which values for B_D and $\langle D^0 \rangle_z$ are extracted with the formula given, for example, by Berne and Pecora[22] for the concentration dependence:

$$\langle D^e \rangle_z \approx \langle D^0 \rangle_z (1 + (2MB_2 - C_2)c) \equiv \langle D^0 \rangle_z (1 + B_D c) \quad \text{(II.12)}$$

Here C_2 is the coefficient in the virial expansion[23,24]

$$f \approx f^0(1 + C_2 c) \quad \text{(II.13)}$$

for the friction coefficient.

The quantity B_D is plotted vs. $1/I$ in Figure 10 and is discussed later. The quantity $\langle D^0 \rangle_z$ is found to have the value

$$\langle D^0 \rangle_z = (0.90 \pm 0.06) \times 10^{-11} \text{ m}^2/\text{s} \quad \text{(II.14)}$$

independent of I.

We next consider the shape of the correlation function. From Figure 5 we see that for low ionic strength and high concentration the curves for ln $(b^{1/2}|g^{(1)}(q,\tau)|)$ show an initial decay followed by a tail. This time evolution resembles that found by Dalberg et al.,[8] Brown et al.,[25] and Pusey[26] for strongly interacting polystyrene spheres.

Since in our case q^{-1} is much larger than the average nearest-neighbor distance, R_m, we are in the regime where correlated motions are important. This many-body problem makes even qualitative discussion of the long-time behavior difficult. However, the similarity of our data obtained for $q^{-1} > R_m$ and those of ref 8 and 26 for $q^{-1} <$

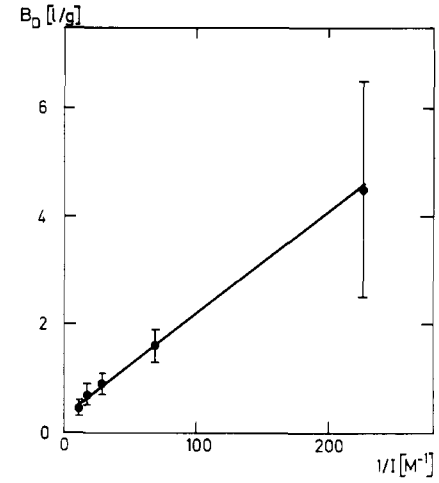

Figure 10. Diffusion virial coefficient as a function of $1/I$. The error bars include conservatively assessed systematic errors and hence the straight line drawn by eye is inside all the bars.

R_m may be helpful. As pointed out by Pusey,[26] when $q^{-1} > R_m$ and the data for $q^{-1} < R_m$ are similar to those for $q^{-1} > R_m$, the Vineyard[27] approximation

$$F(q,\tau) = S(q)F_S(q,\tau) \quad \text{(II.15)}$$

might apply. Here, $F(q,\tau)$ is the coherent intermediate scattering function,[26] $F_S(q,\tau)$ is the self intermediate scattering, SIS, function,[26] and $S(q)$ is the static structure factor.[25] This approximation (eq II.15) does not correctly describe the initial behavior since structural narrowing giving $D^e \propto S^{-1}(q)$[28] is neglected.

Introducing the so-called cage model, Dalberg et al.[8] derived an expression for $F_S(q,\tau)$ which they used in conjunction with eq II.15. According to this model, each particle is enclosed in an average potential well or cage set up by its nearest neighbors. The diffusion is then characterized by the average diffusion coefficients $\langle D^P \rangle$ and $\langle D^C \rangle$ of the particle and cage, respectively. Assuming the particle to be "trapped" in a harmonic oscillator potential, we can then set[8]

$$F_S(q,\tau) = F_S^P(q,\tau)F_S^C(q,\tau) \quad \text{(II.16)}$$

where

$$F_S^P(q,\tau) = \exp[-\langle D^P \rangle q^2 t_0(1 - \exp(-\tau/t_0))] \quad \text{(II.17)}$$

and

$$F_S^C(q,\tau) = \exp[-\langle D^C \rangle q^2 \tau] \quad \text{(II.18)}$$

are the SIS functions for the particle and the cage, respectively, and t_0 is a measure of the transit time of the particle through the cage.

A fit to experimental data then yields values for $\langle D^P \rangle$, $\langle D^C \rangle$, and t_0. In particular, we have

$$\langle D^e \rangle = \langle D^P \rangle + \langle D^C \rangle \quad \text{(II.19)}$$

For $\tau \gg t_0$ the SIS function for the particle becomes independent of τ

$$F_S^P(q,\tau) \approx \exp[-\langle D^P \rangle q^2 t_0] \quad \text{(II.20)}$$

An approach similar to that of Dalberg et al.[8] was used by Pusey.[26] Details concerning the similarity and difference between these two models are given in ref 8 and 26.

III. Discussion

Polydispersity. It is argued in section II that the value of the quantity $\langle D^e \rangle_z^{-1} \partial(\langle \Gamma \rangle / q^2)/\partial q^2$ is entirely due to

polydispersity. Combining eq II.8 and II.10 then yields

$$\frac{1}{3}\left[\langle R_G^2\rangle_z - \frac{\langle D^e R_G^2\rangle_z}{\langle D^e\rangle_z}\right] = (3.1 \pm 0.5) \times 10^{-16}\ \mathrm{m}^2 \quad \text{(III.1)}$$

Using the value of $\langle R_G^2\rangle_z$ obtained from the static measurements and assuming the equivalent-sphere parameter ξ_f defined by the relation[6]

$$D^0 \equiv k_B T/6\pi\eta\xi_f R_G \quad \text{(III.2)}$$

to be independent of R_G, we obtain from eq III.1 and II.11

$$\langle R_G^2\rangle_z = (1.6 \pm 0.3)\frac{\langle R_G\rangle_z}{\langle 1/R_G\rangle_z} \quad \text{(III.3)}$$

and

$$\langle 1/R_G^2\rangle_z = (1.6 \pm 0.1)\langle 1/R_G\rangle_z^2 \quad \text{(III.4)}$$

To obtain a relationship between moments in the number-average of R_G we introduce the random coil relationship $R_G \propto M^{1/2}$.[29] This relationship is found to be valid for sodium alginate in 0.1 N NaCl by ref 3 and 10, which both obtained $a = 0.5$ for the exponent in the relationship $R_G \propto M^a$. As discussed below, the reason for this low value is that the excluded volume effect for alginate molecules is small since they are highly extended due to hindered rotation.[1] In section II we have found $\langle R_G^2\rangle_z^{1/2}$, within uncertainty, to be independent of I for our four highest ionic strengths. We later present arguments in favor of such a result. This suggests that the constant a also is independent of I in the region 14–95 mM. In any case, if a is slightly higher than 0.5, that will not significantly alter our results. Equations III.3 and III.4 may then be written as

$$S_1 \equiv \frac{\langle R_G^6\rangle_n\langle R_G^3\rangle_n}{\langle R_G^5\rangle_n\langle R_G^4\rangle_n} = 1.6 \pm 0.3 \quad \text{(III.5)}$$

and

$$S_2 \equiv \frac{\langle R_G^4\rangle_n\langle R_G^2\rangle_n}{\langle R_G^3\rangle_n\langle R_G^3\rangle_n} = 1.6 \pm 0.1 \quad \text{(III.6)}$$

It is interesting to compare these experimental values for S_1 and S_2 with those for a Schulz molecular weight distribution,[4,5] which has been widely used for cellulosic materials.[10] For all adjustable parameters in that distribution one finds $S_1 \leq 4/3$ and $S_2 \leq 4/\pi$ and hence this distribution cannot be fitted to our experimental data. Dingsøyr[3] has also obtained results for sodium alginate solutions which do not fit a Schulz distribution.

The ratios $\langle M\rangle_z/\langle M\rangle_w$ and $\langle M\rangle_w/\langle M\rangle_n$ are quite often used to characterize the polydispersity.[3,10] By using the relation $R_G \propto M^{1/2}$ in conjunction with the Schwarz inequality,[30] it can be shown that[20]

$$4.1 \pm 1.6 = S_1^2 S_2 \geq \langle M\rangle_z/\langle M\rangle_w \geq S_1 S_2 = 2.6 \pm 0.5 \quad \text{(III.7)}$$

and

$$\langle M\rangle_w/\langle M\rangle_n \geq S_2 = 1.6 \pm 0.1 \quad \text{(III.8)}$$

These results are in reasonable agreement with the value[10] $\langle M\rangle_w/\langle M\rangle_n = 3$ and the limits[3] $\langle M\rangle_z/\langle M\rangle_w \geq 2.2$ and $\langle M\rangle_w/\langle M\rangle_n \geq 2.5$ as obtained with experimental methods different from those of the present work.

We also introduce the ratios

$$Q_1 = \langle R_G^2\rangle_z^{1/2}\langle 1/R_G\rangle_z \quad \text{(III.9)}$$

and

$$Q_2 = \left(\frac{\langle R_G^2\rangle_z^{3/2}/\langle M\rangle_w}{\langle R_G^3/M\rangle_w}\right)^{1/3} \quad \text{(III.10)}$$

which are used later in this section. According to ref 20, these ratios are expressed by means of S_1 and S_2 as

$$1.3 \pm 0.1 = S_1^{1/2} \leq Q_1 \leq S_1 = 1.7 \pm 0.3$$

or

$$Q_1 = 1.6 \pm 0.4 \quad \text{(III.11)}$$

and

$$1.7 \pm 0.2 = S_1^{1/2}S_2^{2/3} \leq Q_2 \leq S_1 S_2^{2/3} = 2.2 \pm 0.4$$

or

$$Q_2 = 2.1 \pm 0.6 \quad \text{(III.12)}$$

Interaction Effects. In the following we discuss the values for B_2 (see Figure 3) and B_D (see Figure 10) and the leveling off in the highest concentration range of $Kc/R(0)$ (see Figure 2) and of $\langle D^e\rangle_z$ (see Figure 9).

Let us first consider B_2 (we ignore polydispersity). Figure 3 shows that in the ionic strength region examined in the present work B_2 is always positive, reflecting repulsion between negatively charged alginate ions. The increase in B_2 with decreasing I is then a result of an increase in the Debye–Hückel screening length. This can be expressed in a more quantitative way as follows. According to Nagasawa and Takahashi,[7] when the polymer solution is dialyzed to equilibrium with a salt of univalent[49] ions, the following expression is a general one:

$$B_2 = \frac{Z^2 K_1 K_2}{4M^2 I} \quad \text{(III.13)}$$

Here, Z is the number of charges of the polymer ion and K_1 and K_2 are correction factors due to electrostatic interaction and the chain character of the macroion, respectively. In Figure 3 the straight line through the experimental points is given by

$$2B_2M = 1.0 + 0.071/I \quad \text{(III.14)}$$

where $2B_2M$ is in L/g and I is in M. The presence of a constant term in this equation is not in contradiction to the absence of a constant term in eq III.13 as K_2 in that equation may depend on I for high ionic strengths. Comparing eq III.13 and III.14 yields

$$K_1 K_2 = (2.9 \pm 0.6) \times 10^{-2} \quad \text{(III.15)}$$

Assuming $K_2 = 1$ and $K_1 = (Z_{eff}/Z)^2$,[3,31] where Z_{eff} is the effective charge number of the polymer ion, we obtain $Z_{eff}/Z = 0.17 \pm 0.02$. This value is considerably lower than the value 0.6 found by Buchner et al.[32] from electrical conductance and transference measurements and the values 0.40 ± 0.05 and 0.29 ± 0.05 obtained by Katchalsky et al.[33] from Donnan equilibrium and osmotic pressure measurements, respectively. These results indicate that K_2 is considerably less than 1 and that nonideality due to the chain character of the alginate molecule must also be taken into account. According to ref 7, nonideality is to be expected in the I region examined in the present work. However, it must be emphasized that polydispersity, which has not been taken into account, may also lower the value of B_2.

We next consider the virial coefficient B_D. As seen from Figure 10, B_D also varies linearly with $1/I$. The straight line in the figure is given by

$$B_D = 0.32 + 0.019/I \quad \text{(III.16)}$$

The coefficient B_D is, according to eq II.12, related to B_2 by $B_D \equiv 2MB_2 - C_2$, where C_2 is the frictional virial coefficient. Inserting eq III.14 and III.16 into this relation, we then obtain

$$C_2 = 0.68 + 0.052/I \quad \text{(III.17)}$$

Hence, C_2 is always positive as has been pointed out by Tanford.[34]

We finally consider the leveling off of $Kc/R(0)$ and $\langle D^e \rangle_z$. This leveling off of the former is not due to the influence of higher order terms in the virial expansion (see eq II.4) since they are all positive for repulsive interaction.[35] The following explanation may be a reasonable one.

It has been shown that sodium alginate is fully dissociated at pH 6.3.[2] Using the value 198 for the molecular weight of the monomer unit,[10] we then find that a sodium alginate solution with concentration 2 g/L will contain 10 mM Na^+ counterions. A large fraction of them will, however, be fixed to the alginate anions.[32,33] Nevertheless, due to the free counterions the Debye–Hückel screening length and thus the virial coefficients will decrease with increasing alginate concentration. Furthermore, polydispersity, which is not incorporated in the theory for the virial expansion of ref 35, may also cause the value of $Kc/R(0)$ to level off at high c.

The deviation from linearity in $\langle D^e \rangle_z$ may be due to the same effects. However, the behavior of this quantity may also be affected by changes in the friction coefficient, which in this concentration region is probably not properly described by a first-order expansion in c.

Shape of the Correlation Functions. Before applying the model of Dalberg et al.[8] referred to in section II, we make the following remarks. Bimodal decays are also observed[36–41] in systems for which the shape of the correlation function is explained by entanglement coupling. At the lowest ionic strengths and the highest concentrations in the present work it is difficult to evaluate to which degree entanglement effects influence the shape of the correlation functions. For other macromolecular systems[37,39,41] it has been observed that there is a critical concentration above which the fast decay constant increases rapidly with c. This is attributed to entanglement effects. Such a behavior is not observed for the present system, where the fast decay constant shows an initial fast increase followed by a leveling off at the highest concentrations. This does not, however, preclude entirely the possibility of the presence of entanglement effects.

It is also difficult to determine which interaction type is the main source for the slow component in the decay of the correlation function. It may be that we have some degree of entanglement and that knots must be untied before molecules can move greater distances. It is to be expected that when R_G is unchanged, entanglement effects should not increase with increasing repulsive electrostatic interaction. As seen from Figure 5 we have a significant contribution from a slow component both at 4.4 mM and at 14 mM, where the electrostatic interaction is strong. In the latter case we found the value of R_G to be equal that at 95 mM, where the electrostatic interaction is weak and where we have practically no slow component present (see Figure 5c). Hence, it appears that entanglement effects are not the main source for the slow component. Below we shall see that we may interpret the shapes of the correlation functions by means of electrostatic interaction.

In Figure 5 we see that the ionic strength has a small effect on the shape at low concentration. This may be expected since here the interparticle distances are large

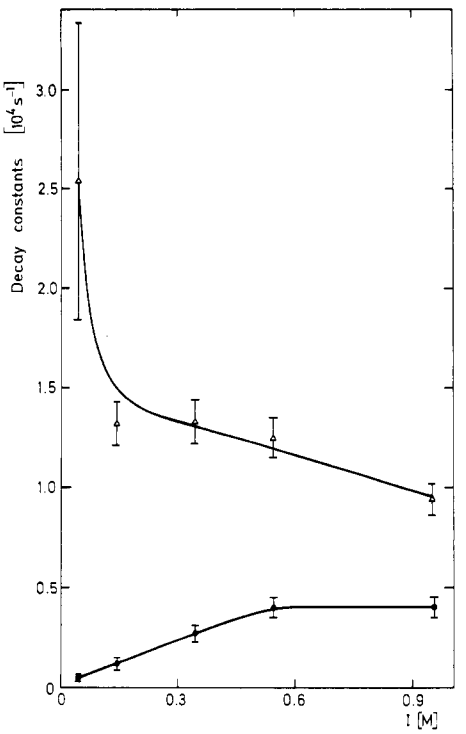

Figure 11. $\langle \Gamma \rangle$ (△) and $\langle \Gamma(90\ \mu s) \rangle$ (●) as a function of I for $\theta = 90°$ and $c = 1.8$ g/L. The error bars include conservatively assessed systematic errors. The smooth curves are drawn by eye.

and hence the electrostatic particle interactions are weak.

At the highest concentrations the decay constants $\langle \Gamma \rangle$ and $\langle \Gamma(90\ \mu s) \rangle$, respectively, decrease and increase with increasing ionic strength as demonstrated in Figure 11. The decrease in $\langle \Gamma \rangle$ is due to decreased electrostatic interaction. The behavior of $\langle \Gamma(90\ \mu s) \rangle$ may be understood in the framework of the cage model[8] as outlined in section II. According to this model, the range of interaction, and thus the number of particles, decreases and hence $\langle \Gamma(90\ \mu s) \rangle$ increases with increasing I.

In the following we only analyze the data obtained at the lowest ionic strength, where the electrostatic interaction is strongest and the cage model may be applicable over a large concentration range. Let us first consider the diffusion coefficient $\langle D^C \rangle$ of the cage as given by the experimental quantity $\langle \Gamma(\tau_0) \rangle / q^2$. When $\langle \Gamma(\tau_0) \rangle / q^2$ was evaluated at $\tau_0 = 130\ \mu s$, we found the value for that quantity to be independent of q^2. In Figure 12 we have plotted $\langle D^C \rangle$ vs. c, evaluated at $\tau_0 = 130\ \mu s$ and $\theta = 90°$. The straight line in that plot corresponds to

$$\langle D^C \rangle \propto c^{\nu_D} \quad \text{(III.18)}$$

with $\nu_D = -0.7 \pm 0.1$. It is interesting to note that when the "size" of the cage is independent of concentration, the number of particles in the cage is proportional to c and $\nu_D = -1$.[42] However, it is to be expected that the Debye–Hückel screening length and hence the size will decrease with increasing c and therefore $\nu_D < -1$.

The value for the ratio $\langle D^0 \rangle_z / \langle D^C \rangle$ is found to be 8.3 ± 3.6 at the highest concentration ($c = 1.9$ g/L) and 1.6 ± 0.7 at the lowest concentration ($c = 0.16$ g/L). Due to the high polydispersity in our samples we cannot, as suggested by Dalberg et al.,[8] set the values of this ratio equal to the number of particles participating in the formation of a cage. However, the value 1.6 ± 0.7 of the ratio $\langle D^0 \rangle_z / \langle D^C \rangle$ at the lowest concentration means that the contribution from polydispersity to this ratio is less than that value. The ratio 5.2 ± 0.8 between $\langle D^C \rangle$ at $c = 0.16$ g/L and $\langle D^C \rangle$ at $c = 1.9$ g/L then suggests that at least

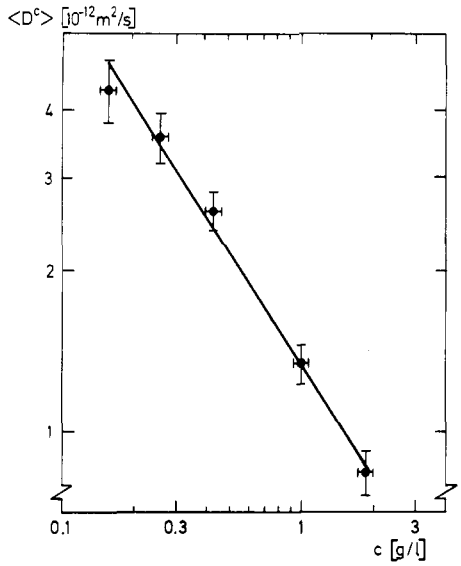

Figure 12. $\langle D^C \rangle = \langle \Gamma(130\ \mu s) \rangle / q^2$ referred to 20 °C plotted vs. concentration for $I = 4.4$ mM and $\theta = 90°$. The error bars include conservatively assessed systematic errors and hence the straight line drawn by eye is within all the bars.

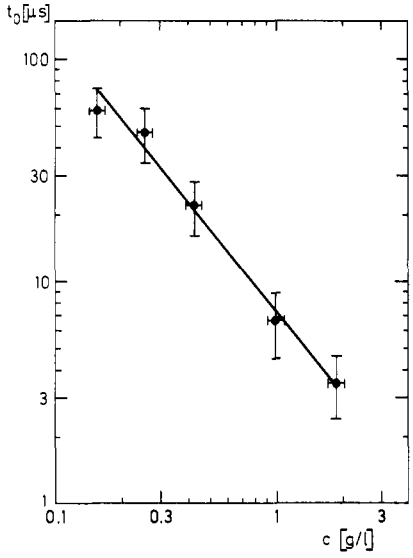

Figure 13. Double-logarithmic plot of t_0 referred to 20 °C vs. concentration for $\theta = 90°$ and $I = 4.4$ mM. The error bars include conservatively assessed systematic errors and hence the straight line drawn by eye is within all the bars.

about 5 particles participate in formation of the cage at the highest concentration.

We next consider the characteristic time, t_0. In Figure 13 values for t_0 are plotted in a double-logarithmic plot. We see that t_0 varies between 3×10^{-6} and 6×10^{-5} s at the highest and lowest concentration, respectively. The straight line in the plot corresponds to

$$t_0 \propto c^{\nu_t} \qquad \text{(III.19)}$$

with $\nu_t = -1.2 \pm 0.2$. This result is in agreement with that of Dalberg et al.,[8] who for strongly interacting polystyrene spheres found the product $t_0 c$ to be approximately independent of c. However, the theoretical explanation for this independence given in ref 8 is not applicable for our samples since the Debye–Hückel screening length here is less than the average center-to-center distance between neighboring particles.

In spite of the above result we cannot give a clear conclusion concerning which type of interaction is causing the bimodal decay. It appears, however, that at the lowest I and highest c region our data are consistent with the notion that an alginate molecule for a short period of time is enclosed within a cage formed by its nearest neighbors. In the following we therefore also analyze our data in a manner which does not involve any assumption of the type of interaction forming the cage.

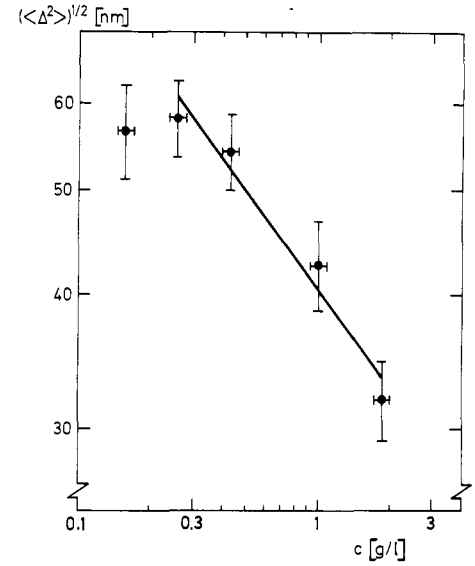

Figure 14. Double-logarithmic plot of $(\langle \Delta^2 \rangle)^{1/2}$ vs. concentration for $\theta = 90°$ and $I = 4.4$ mM. The error bars include conservatively assessed systematic errors. The straight line represents the least-squares fit for the four highest concentrations.

The SIS function for the particle is, in general, given by[43]

$$F_S^P(q,\tau) = \langle \exp(-i\vec{q}\cdot[\vec{r}(t) - \vec{r}(t+\tau)]) \rangle \qquad \text{(III.20)}$$

For $^1/_2\langle(\vec{q}\cdot[\vec{r}(t) - \vec{r}(t+\tau)])^2\rangle \ll 1$, eq III.20 can be approximated by

$$F_S^P(q,\tau) \approx 1 - i\langle \vec{q}\cdot[\vec{r}(t) - \vec{r}(t+\tau)] \rangle - \tfrac{1}{2}\langle(\vec{q}\cdot[\vec{r}(t) - \vec{r}(t+\tau)])^2\rangle \qquad \text{(III.21)}$$

Introducing $\vec{\Delta} \equiv \vec{r}(t) - \vec{r}(t+\tau_L)$, where τ_L is a time much longer than t_0, we write eq III.21 as

$$F_S^P(q,\tau_L) \approx 1 - i\langle \vec{q}\cdot\vec{\Delta} \rangle - \tfrac{1}{2}\langle(\vec{q}\cdot\vec{\Delta})^2\rangle \qquad \text{(III.22)}$$

It is reasonable to assume that $\vec{\Delta}$ is a result of symmetric random motion and hence $\langle \vec{\Delta} \rangle = 0$ and $\langle(\vec{q}\cdot\vec{\Delta})^2\rangle = {}^1/_3 q^2 \cdot \langle \Delta^2 \rangle$. Equation III.22 then reduces to

$$F_S^P(q,\tau_L) \approx 1 - \tfrac{1}{6}q^2\langle \Delta^2 \rangle \approx \exp(-\tfrac{1}{6}q^2\langle \Delta^2 \rangle) \qquad \text{(III.23)}$$

The latter expression suggests $\langle \Delta^2 \rangle = (6/q^2)(i_1 - i_2)$, where experimental values for i_1 are given by the intercept with the $\ln(b^{1/2}|g^{(1)}(q,\tau)|)$ axis of the tangent to the correlation curve at $\tau = 0$ (see Figure 5). Similarly, the value for i_2 is equal to the intercept of the tangent to this curve at $\tau = 130\ \mu s$.

A development quite similar to that above (eq III.20 to III.23) was previously done by Pusey.[26]

In Figure 14, $\langle \Delta^2 \rangle^{1/2}$ is plotted vs. c in a double-logarithmic plot. The straight line in the figure is given by

$$\langle \Delta^2 \rangle^{1/2} \propto c^{\nu_\Delta} \qquad \text{(III.24)}$$

with $\nu_\Delta = -0.30 \pm 0.05$. This is a reasonable value since the average center-to-center distance is proportional to $c^{-1/3}$. The value of $\langle \Delta^2 \rangle^{1/2}$ is about 30 and 60 nm at $c = 1.9$ and 0.16 g/L, respectively. This is to be compared to the average center-to-center distances of 40 and 110 nm, respectively. We notice that the condition $^1/_2\langle(\vec{q}\cdot\vec{\Delta})^2\rangle \ll 1$ used in deriving eq III.23 is indeed fulfilled.

The point for $\langle \Delta^2 \rangle^{1/2}$ at the lowest concentration is outside the straight line in Figure 14. This is not unex-

pected since the cage model is not adequate at this concentration.

Single-Particle Properties. As discussed above, the analysis of the static light scattering data shows the quantity $\langle R_G^2 \rangle_z^{1/2}$ to be independent of I in the region 14–95 mM. It may seem surprising that $\langle R_G^2 \rangle_z^{1/2}$ is independent of I. However, this independence is in agreement with the I independence of $\langle D^0 \rangle_z$ in the region 4.4–95 mM obtained from the dynamic light scattering measurements. Furthermore, in a separate set of experiments we found the intrinsic viscosity, $[\eta]$, to have a rather weak I dependence, ranging from 0.7 ± 0.1 L/g at I = 95 mM to 1.6 ± 0.3 L/g at I = 4.4 mM. Since $[\eta] \propto R_G^3$,[44] this weak I dependence is, within uncertainty, in agreement with the I independence of $\langle R_G^2 \rangle_z^{1/2}$ and $\langle D^0 \rangle_z$. The reason for this small effect of I on the single-particle properties is probably that the alginate molecules due to hindered rotation are highly extended even at infinite ionic strength.[1] In addition, when I varies from 95 to 4.4 mM the Debye–Hückel screening length only varies between 1.0 and 4.5 nm and hence is everywhere lower than the lowest limit for the Kuhn statistical segment obtained below. These results are consistent with the observation made by Smidsrød[1] that the conformation of alginate is much less influenced by ionic strength than other flexible coils.

One important property of a single particle is its extension. For a random coil molecule one usually characterizes such a property by the "Kuhn statistical segment"[45]

$$A_m = 6M_m R_G^2 / b_0 M \qquad \text{(III.25)}$$

where b_0 = 0.515 nm[10] is the length and M_m = 198[10] is the molecular weight of a monomer in the macromolecule. Introducing eq II.5, II.6, and III.7 into eq III.25, we find

$$A_m = 10 \pm 6 \text{ nm} \qquad \text{(III.26)}$$

independent of I in the region 14–95 mM. That value is much lower than the value 34 nm obtained by Smidsrød and Haug[10] for alginate at I = 100 mM when a Schulz distribution was assumed.

Using our values for $\langle D^0 \rangle_z$ and $\langle R_G^2 \rangle_z^{1/2}$ in conjunction with eq III.11, we find the following value for the parameter ξ_f in eq III.2:

$$\xi_f = 0.75 \pm 0.25 \qquad \text{(III.27)}$$

This value is in agreement with the value ξ_f = 0.665 as predicted by the Kirkwood–Riseman theory[46] for a molecule with a large number of segments.

For a polydisperse solution of flexible coils, using the concept of equivalent hydrodynamic spheres, the intrinsic viscosity, $[\eta]$, is given by[44]

$$[\eta] = \frac{10}{3}\pi N_A \xi_V^3 \left\langle \frac{R_G^3}{M} \right\rangle_w \qquad \text{(III.28)}$$

where ξ_V is an equivalent-sphere parameter for viscosity. Introducing our values for $[\eta]$, $\langle R_G^2 \rangle_z^{1/2}$, and $\langle M \rangle_w$ and eq III.12 into eq III.28, we find at 95 mM

$$\xi_V = 1.15 \pm 0.35 \qquad \text{(III.29)}$$

and at 14 mM

$$\xi_V = 1.3 \pm 0.4 \qquad \text{(III.30)}$$

These values are in poor agreement with the values ξ_V = 0.62 and ξ_V = 0.43 obtained by Smidsrød[47] at I = 100 mM and $M_w = 2.7 \times 10^6$ and $M_w = 1.1 \times 10^5$, respectively. As in the case for the Kuhn statistical segment, this disagreement is mainly due to the fact that Smidsrød has assumed at Schulz distribution. Our value for ξ_V is, within the large error, in agreement with the value 0.875 as predicted by the Kirkwood–Riseman theory[46] and also with a number of experimental values obtained for other types of flexible coils.[48]

IV. Conclusion

In investigating polydisperse macromolecular systems the combination of static and dynamic light scattering is quite a powerful tool. There are, however, experimental problems due to scattering from dust, which contributes significantly to the assessed large uncertainties. This effect may be reduced directly by a more efficient filtering procedure or indirectly by electronically blocking the signal when dust enters the scattering volume. The interpretation of the data is hampered by the fact that there is a lack of an adequate theory which takes both polydispersity and particle interaction into account. Finally, the alginate molecule has a complex structure. Hence, we had to introduce certain simplifications and models by which our data could be analyzed in a consistent way.

In the analysis of the polydispersity we made use of the relationships $R_G \propto M^{1/2}$[3,10] and $D \propto 1/R_G$.[46] Furthermore, we obtained values for the q^2 dependence of the mean and the variance of the effective diffusion coefficient D^e, which may be ascribed to the effect of polydispersity. Then, by the introduction of the Schwarz inequality, upper and lower limits were obtained for ratios consisting of various moments of the radius of gyration and the molecular weight. The molecular weight distribution does not fit that of Schulz.[4,5]

The following single-particle properties were found: $\langle M \rangle_w = (1.9 \pm 0.2) \times 10^5$, $\langle R_G^2 \rangle_z^{1/2} = 50 \pm 7$ nm, $\langle D^0 \rangle_z = (0.90 \pm 0.06) \times 10^{-11}$ m²/s (at 20 °C), and $\xi_f = 0.75 \pm 0.25$. All these quantities are independent of ionic strength in the examined region, perhaps due to the fact that the alginate molecules are extended and open.

For the parameter ξ_V we obtained the values 1.15 ± 0.35 and 1.3 ± 0.4 at I = 95 mM and I = 14 mM, respectively. Both values are considerably higher than what was reported in ref 47 but are in agreement with the Kirkwood–Riseman model.[46] This suggests, therefore, that the alginate molecules are not free drained. However, due to the large uncertainty in our values for ξ_f and ξ_V the agreement with the Kirkwood–Riseman model does not imply that this model gives a correct description of the alginate molecules.

Consistent with the above results is our value 10 ± 6 nm for the Kuhn statistical segment, which is considerably lower than the value 34 nm given in ref 10. Hence, the alginate molecules are very extended but substantially less than what was earlier believed.

In the analysis of the interaction properties as reflected in the virial coefficients and the shapes of the photon correlation functions, we have ignored the effects of polydispersity. The ionic strength dependence and the values of the static virial coefficient are in reasonable agreement with existing theories for monodisperse systems. The data suggest a large degree of nonideality due to the chain character of the alginate. For the diffusion virial coefficient there do not exist theoretical predictions with which our data could be compared.

At the lowest ionic strength (4.4 mM), where the interparticle interaction is strong, the shapes of the correlation functions were analyzed by using the cage model.[8] A characteristic particle diffusion distance Δ was introduced, the root-mean-square value of which was found to be proportional to the inverse value of the interparticle distance. The "size" of the cage decreases slightly with concentration. At the highest concentration (2 g/L) there appears to be about five molecules within that cage for a short period of time ($\sim 10^{-5}$ s). The I dependence of the

shape of the correlation function seems to indicate that electrostatic interaction is the main source for the bimodal decay at low ionic strength.

Acknowledgment. We wish to express our gratitude to the Royal Norwegian Council for Sciences and Humanities for financial support.

References and Notes

(1) Smidsrød, O. Report No. 34, Norwegian Institute of Seaweed Research, Trondheim, Norway, 1973.
(2) Haug, A. Report No. 30, Norwegian Institute of Seaweed Research, Trondheim, Norway, 1964.
(3) Dingsøyr, E. "Light Scattering Properties of Alginate", Lic. techn. thesis, University of Trondheim, Norway, 1974.
(4) Chu, B. "Laser Light Scattering"; Academic Press: New York, 1974; p 230.
(5) Zimm, B. H. *J. Chem. Phys.* **1948**, *16*, 1099.
(6) Tanford, C. "Physical Chemistry of Macromolecules"; Wiley: New York, 1961; pp 344–349.
(7) Nagasawa, M.; Takahashi, A. In "Light Scattering from Polymer Solutions"; Huglin, M. B., Ed.; Academic Press: New York, 1972.
(8) Dalberg, P. S.; Bøe, A.; Strand, K. A.; Sikkeland, T. *J. Chem. Phys.* **1978**, *69*, 5473.
(9) Grasdalen, H.; Larsen, B.; Smidsrød, O. *Carbohydr. Res.* **1977**, *56*, C11.
(10) Smidsrød, O.; Haug, A. *Acta Chem. Scand.* **1968**, *22*, 797.
(11) Dingsøyr, E.; Smidsrød, O. *Br. Polym. J.* **1977**, *9*, 56.
(12) Brice, B. A.; Halwer, M.; Speiser, R. *J. Opt. Soc. Am.* **1950**, *40*, 768.
(13) Zimm, B. H. *J. Chem. Phys.* **1948**, *16*, 1093.
(14) Reference 6, Chapter V.
(15) Reference 6, p 303.
(16) Jakeman, E. In "Photon Correlation and Light Beating Spectroscopy"; Cummins, H. Z., Pike, E. R., Eds.; Plenum Press: New York, 1974.
(17) Raj, R.; Flygare, W. H. *Biochemistry* **1974**, *13*, 3336.
(18) Gordon, J. P.; Leite, R. C. C.; Moore, R. S.; Porto, S. P. S.; Whinnery, J. R. *J. Appl. Phys.* **1965**, *36*, 3.
(19) Brehm, G. A.; Bloomfield, V. A. *Macromolecules* **1975**, *8*, 663.
(20) Strand, K. A.; Sikkeland, T., in preparation.
(21) Berne, B. J.; Pecora, R. "Dynamic Light Scattering"; Wiley: New York, 1976; Chapter 8.8.
(22) Reference 21, Chapter 13.5.
(23) Pyun, C. W.; Fixman, M. *J. Chem. Phys.* **1964**, *41*, 937.
(24) Cummins, H. Z. In ref 16.
(25) Brown, J. C.; Pusey, P. N.; Goodwin, J. W.; Ottewill, R. H. *J. Phys. A* **1975**, *8*, 664.
(26) Pusey, P. N. *J. Phys. A* **1978**, *11*, 119.
(27) Vineyard, G. H. *Phys. Rev.* **1978**, *110*, 999.
(28) Pusey, P. N. *J. Phys. A* **1975**, *8*, 1433.
(29) Reference 6, p 158.
(30) Byron, F. W.; Fuller, R. W. "Mathematics of Classical and Quantum Physics"; Addison-Wesley: New York, 1969; p 148.
(31) Inagaki, H.; Oda, T. *Makromol. Chem.* **1956**, *21*, 1.
(32) Buchner, P.; Cooper, R. E.; Wassermann, A. *J. Chem. Soc.* **1961**, 3974.
(33) Katchalsky, A.; Cooper, R. E.; Updahyay, J.; Wassermann, A. *J. Chem. Soc.* **1961**, 5198.
(34) Reference 6, p 372.
(35) Stockmayer, W. H.; Casassa, E. F. *J. Chem. Phys.* **1952**, *20*, 1560.
(36) Adam, M.; Delsanti, M.; Jannik, G. *J. Phys., Lett. (Paris)* **1976**, *37*, 53.
(37) Adam, M.; Delsanti, M. *Macromolecules* **1977**, *10*, 1229.
(38) Lee, W. I.; Schmitz, K. S.; Lin, S. C.; Schurr, J. M. *Biopolymers* **1977**, *16*, 583.
(39) Munch, J. P.; Candau, S.; Herz, J.; Hild, G. *J. Phys. (Paris)* **1977**, *38*, 91.
(40) Matiez, P.; Weisbuch, G.; Mouttet, C. *Biopolymers* **1979**, *18*, 1465.
(41) Matiez, P.; Mouttet, C.; Weisbuch, G. *J. Phys. (Paris)* **1980**, *41*, 519.
(42) Reference 21, Chapter 13.7.
(43) Reference 21, Chapter 5.6.
(44) Flory, P. J. "Principles of Polymer Chemistry"; Cornell University Press: Ithaca, N.Y., 1953; Chapter XIV.
(45) Reference 6, p 159.
(46) Kirkwood, J. G.; Riseman, J. *J. Chem. Phys.* **1948**, *16*, 565.
(47) Smidsrød, O. *Carbohydr. Res.* **1970**, *13*, 359.
(48) Reference 6, p 401.
(49) It is straightforward to show that this expression also is valid for multivalent ions.

Angular Scattering Functions for Subchains Defined by a Generator Matrix Treatment of Simple Chains with Excluded Volume

Wayne L. Mattice

Department of Chemistry, Louisiana State University, Baton Rouge, Louisiana 70803.
Received November 13, 1981

ABSTRACT: Angular scattering functions, $P(\mu)$, have been computed for subchains located in the middle and at the end of a polymethylene chain. The rotational isomeric state model developed by Flory and co-workers is used for the unperturbed chain. Chain expansion is introduced using a matrix treatment which satisfactorily reproduces several configuration-dependent properties of macromolecules perturbed by long-range interactions. At low angles $P(\mu)$ for subchains in perturbed chains depends on subchain location. This observation simply demonstrates that the mean-square radius of gyration, $\langle s^2 \rangle$, of a perturbed subchain depends on the location of that subchain within the main chain, as expected. Additional effects, arising from further differences in the distribution of chain atoms in perturbed subchains, are apparent at larger angles when $1/P(\mu)$ is examined as a function of $\langle s^2 \rangle \mu^2$. The excluded volume effect produces an increase in $P(\mu)$ for subchains at large $\langle s^2 \rangle \mu^2$. However, subchain location dependence of $P(\mu)$ for perturbed chains occurs only when $\langle s^2 \rangle \mu^2$ is so large that $P(\mu)$ itself is quite small.

Generator matrix methods have been widely used to evaluate the statistical mechanical average of configuration-dependent physical properties of chain molecules unperturbed by long-range intramolecular interactions.[1] These calculations permit a realistic treatment of a chain molecule because they utilize the bond lengths, bond angles, and short-range contributions to torsional potentials appropriate for the polymer in question. Recently generator matrix methods have been devised which permit rapid computation of a reasonable approximation to average configuration-dependent physical properties of chains significantly perturbed by long-range intramolecular interactions.[2-4] Bond lengths, bond angles, and short-range contributions to the torsional potentials are retained at the

0024-9297/82/2215-0579$01.25/0